Introducing Lyapunov profiles of cellular automata

JAN M. BAETENS[1]⋆, JANKO GRAVNER[2]

[1] *KERMIT, Department of Mathematical Modelling, Statistics and Bioinformatics, Ghent University, Coupure links 653, Gent, Belgium*
[2] *Mathematics Department, University of California, Davis, CA 95616, USA*

Received XX; In final form YY

Motivated by their important role in smooth dynamical systems, Lyapunov exponents have been conceived decades ago as a means to study the stability of cellular automata (CAs). More precisely, they quantify their sensitive dependence on initial conditions. As a next step towards the establishment of a dynamical systems theory of CAs that is inspired by its analogue for smooth dynamical systems, we introduce the concept of Lyapunov profiles of CAs. These constructs may be considered analogous to the Lyapunov spectra of higher-dimensional smooth dynamical systems. Doing so, we unify the competing approaches to Lyapunov exponents of CAs, as Lyapunov profiles capture both the spreading properties of a set of defects and the exponential accumulation rates of defects within this set.

Key words: cellular automata; damage front; Lyapunov exponents; Lyapunov spectrum; stability

1 INTRODUCTION

In spite of their intrinsic simplicity, cellular automata (CAs) [24] have been proven to be capable of evolving intriguing spatio-temporal dynamics [12, 14, 26]. Moreover, they are increasingly appreciated as full-fledged models for

⋆ email: jan.baetens@ugent.be

mimicking complex biological and physical processes [19, 20], and one may expect that their importance will increase in the near future as GPU architectures are especially suited to run CA-based models [13]. For these reasons, it is important to have a full understanding of CA behaviour, and how it is affected by design parameters such as the update rule, the synchronism, the underlying topology, or the neighbourhood structure. For the sake of reproducibility and objectivity, quantitative tools are especially useful because they allow to express how the behaviour of a CA is affected by changes of its design parameters. Throughout the past two decades many measures have been proposed to grasp the dynamical properties of CAs, such as the Langton parameter [17], Lyapunov exponents [5, 8, 21] entropies and dimensions [16] and others [27]; another tool are mean-field approximations [10]. A comprehensive overview of approaches to the classification of CAs can be found in [18].

Inspired by the established formalism in the case of smooth dynamical systems, the Lyapunov exponents of CAs have received considerable attention, through two distinct viewpoints. The first one identifies Lyapunov exponents of one-dimensional CAs with the rates by which the damage front moves to the right and to the left starting from an initial perturbation, and has been adopted by several authors [8, 11, 22], after their formalization by Shereshevsky [21]. According to this viewpoint, every one-dimensional CA and every finite initial perturbation generate two exponents, one for each direction, whose equality implies that the rate of damage spread is symmetric. An alternative viewpoint was put forward by Bagnoli et al. [5] and involves a single Lyapunov exponent for every CA. This quantity is the exponential rate by which defects accumulate if the CA is evolved for a long time from an initial configuration on a finite set with a single defect [4, 5]. Consequently, it fails to capture the spatial aspect of damage propagation. Therefore, the two approaches to Lyapunov exponents seemingly have little in common.

Since Lyapunov exponents in the viewpoint of Bagnoli et al. [5] quantify the accumulation of defects, they give insight into the intensity of the defect propagation, whereas the constructs formalized by Shereshevsky [21] indicate how fast the damage front widens as the CA evolves. An approach which would integrate both aspects in a unifying concept would introduce a new perspective on stability of CAs.

This paper proposes a unification of the two competing viewpoints through the so-called Lyapunov profile, which may be understood informally as the counterpart of the Lyapunov spectrum of smooth dynamical systems. These profiles capture the spreading properties of a set of defects, as well as the

exponential accumulation rates of defects within this set. In this paper we present an intuitive and mostly informal introduction to Lyapunov profiles. For a more detailed rigorous and computational approach, we refer the reader to [3]. After introducing the rationale behind these profiles together with their definition in Section 2, we will present a comprehensive study of the Lyapunov profiles of elementary CAs (ECAs) in Section 3, and investigate to what extent these can be rhymed with existing CA classifications.

2 LYAPUNOV PROFILES OF CELLULAR AUTOMATA

2.1 Rationale

The easiest way to conceptualize Lyapunov profiles is to start from the notion of Lyapunov exponents of CAs proposed by Bagnoli et al. [5]. These authors introduce the accumulation of defects, which we now informally describe (see (2) for a formal definition). Any defect present at a site y at time t generates a defect at a neighboring site x at time $t+1$ if flipping the CA state at time t at y results in a different state at x than assigned by the CA dynamics at time $t+1$. We emphasize that the defect dynamics interacts with the CA evolution but does not affect it, so the values assigned by the CA are unchanged. A site may contain any nonnegative number of defects, and each defect acts independently of others. By default, we begin by a single defect at the origin at time 0. Subsequently, we track the total number of defects as the Boolean CA evolves, and the resulting Lyapunov exponent in the sense of Bagnoli et al. [5] is the time-averaged exponential rate by which the number of defects grows. More formally, we have:

$$\lambda = \lim_{t\to\infty} \frac{1}{t} \log\left(\frac{\epsilon_t}{\epsilon_0}\right) , \tag{1}$$

where ϵ_t denotes the total number of defects at the t-th step. We refer to [1] for an algorithm to track ϵ_t, as it suffices for our purpose to point out the fact that both the position and multiplicity of defects need to be recorded as the CA evolves over time. Yet, it is clear from (1) that this information is lost when computing the Lyapunov exponent in the sense of Bagnoli et al. [5]. This information can, however, be accessed by introducing the vector Δ_t whose i-th element is the number of defects in cell c_i at a given step. In this way, we track both the multiplicity and position of defects. It should be mentioned at this point that Bagnoli et al. [5] refer to the quantity given by (1) as the maximum Lyapunov exponent (MLE) of a CA. This terminology is very ambiguous since it is used in the case of smooth dynamical systems

to identify the largest exponent in the Lyapunov spectrum, whereas Bagnoli et al. [5] define a single quantity, the sum of defects across all dimensions in phase space.

By explicitly tracking the vector Δ_t, we envision a CA consisting of n cells as an n-dimensional system, where every cell of a one-dimensional array makes up one dimension. Continuing along this line of reasoning, it becomes obvious that tracking the vector Δ_t allows us to assess how perturbations are amplified along any direction in the phase space of a CA. More precisely, the i-th element in this vector gives information on how fast defects propagate along the i-th dimension of a CA's phase space, i.e. in its i-th cell. Loosely speaking, properly normalized, Δ_t may be understood as the Lyapunov profile of a CA for large t. In the remainder of this section, a more formal definition will be given of this construct.

2.2 Formalizing Lyapunov profiles

Throughout the remainder of this paper we consider binary CAs on a 1-dimensional integer lattice $\mathbb{Z}$ with state space $\{0, 1\}$. Assuming that the neighborhood $\mathcal{N} \subset \mathbb{Z}$ is $[-r,\, r]$, their dynamics is governed by a local update function of $2\,r + 1$ variables: $\phi : \{0, 1\}^{2\,r+1} \to \{0, 1\}$. The neighborhood of a point $x \in \mathbb{Z}$ is the translation $\mathcal{N}_x = x + \mathcal{N} = [x - r,\, x + r]$. Globally, an update function $\Phi : \{0, 1\}^{\mathbb{Z}} \to \{0, 1\}^{\mathbb{Z}}$ governs the dynamics as follows:

$$\Phi(\eta)(x) = \phi(\eta(x-r), \eta(x-r+1), \ldots, \eta(x), \ldots, \eta(x+r-1), \eta(x+r))\,,$$

where $\eta \in \{0, 1\}^{\mathbb{Z}}$, and $x \in \mathbb{Z}$ are arbitrary. A trajectory of the CA starting from a fixed (deterministic or random) initial configuration ξ_0 is denoted as $\xi_t(x) = \xi(x, t)$ for $x \in \mathbb{Z}$ and $t \in \mathbb{Z}_+$.

All the CAs covered in the experimental part of this paper (Section 3) belong to the family of so-called ECAs. They are one-dimensional binary CAs for which $\mathcal{N} = [-1, 1]$, i.e. the state at a given point x is determined by the current state at x and its nearest two neighbors. Given the size of their state space and neighborhood, one can list 256 different update functions for ECAs. These are commonly referred to using the enumeration scheme proposed in [25]. Some noteworthy examples are ECA rules 22, 90 and 150, whose update functions are given by

$$\Phi(\eta)(x) = \eta(x-1) + \eta(x) + \eta(x+1) + \eta(x-1)\,\eta(x)\,\eta(x+1) \mod 2\,,$$

$$\Phi(\eta)(x) = \eta(x-1) + \eta(x+1) \mod 2\,,$$

and

$$\Phi(\eta)(x) = \eta(x-1) + \eta(x) + \eta(x+1) \mod 2\,,$$

respectively. The last two rules are linear (they commute with addition modulo 2), while the first one is not.

The defect propagation properties of a CA do not change if we switch the roles of 0's and 1's or if we make a mirror reflection of the rule. This leaves us with 88 ECA equivalence classes, and we pick a representative one with the smallest Wolfram number from each equivalence class to obtain the 88 minimal ECAs [23].

In order to arrive at a formal definition of the Lyapunov profile of a CA, let us first of all introduce the defect configuration $\Delta_t(x) = \Delta(x,t) \in \mathbb{Z}_+$ that describes the distribution of defects. The defect configuration at the time step $t+1$ is given by:

$$\Delta_{t+1}(x) = \sum_{y \in \mathcal{N}_x} \texttt{change}_t(y,x)\Delta_t(y)\,, \tag{2}$$

where $\texttt{change}_t$ collects the information about effects of perturbations at time t:

$$\texttt{change}_t(y,x) = \begin{cases} 1 & , \quad \text{if } \Phi(\xi_t^{(y)})(x) \neq \xi_{t+1}(x)\,, \\ 0 & , \quad \text{else}\,, \end{cases}$$

with $\xi_t^{(y)}$ the perturbed counterpart of ξ_t at y, which is obtained by flipping the state at y in ξ_t. The initial defect configuration Δ_0 is fixed and assumed to consist of zeros everywhere, except at a single site.

Informally, (2) should be understood as follows. For every $x \in \mathbb{Z}$, $y \in \mathcal{N}_x$, and every defect counted into $\Delta_t(y)$, $\Delta_{t+1}(x)$ is increased by 1 if applying the CA rule on the configuration ξ_t that is perturbed at y results in perturbation at x.

Definition 1. *The Lyapunov profile of a binary, one-dimensional CA is the function $L : \mathbb{R} \to \{-\infty\} \cup [0,\infty)$ given for $\alpha \in \mathbb{R}$ by*

$$L(\alpha) = \lim_{\epsilon \downarrow 0} \limsup_{t \to \infty} \frac{1}{t} \log \left(\sum_{x : |x/t - \alpha| < \epsilon} \Delta(x,t) \right). \tag{3}$$

It can be verified easily that the limit in (3) exists as either a nonnegative finite number or $-\infty$, and that one may replace the sum with maximum.

To understand the above formula, fix a real number α and a small $\epsilon > 0$. As time t increases, the number of defects in the neighborhood $[(\alpha-\epsilon)t, (\alpha+\epsilon)t]$ around αt increases at some exponential rate, that is, this number is about $\exp(L(\alpha,\epsilon)t)$. The rate L clearly depends on both α and ϵ; to remove the

latter dependence, we send $\epsilon \to 0$, which corresponds to a very small linear expansion of the interval around αt. We use $\limsup$ so that the definition applies to the cases when the limit in t fails to exist (even if we are not aware of any such example). The limit in ϵ always exists due to monotonicity.

Given Definition 1, and drawing parallels with the established terminology in works on smooth dynamical systems, we now define the maximal Lyapunov exponent (MLE) as

$$\lambda = \max_{\alpha} L(\alpha). \tag{4}$$

The space-time direction for which the maximum in (4) is achieved, is called the MLE direction, and constitutes the direction with the fastest growing number of defects. This gives a more intuitive definition of the MLE than the one given by Bagnoli et al. [5], though it can be verified empirically that our notion of the MLE is close to the one in [5], if the initial state is the uniform product measure.

The notion of Lyapunov profiles is closely related to the large deviations theory [9], especially as it relates to the spatial accumulation of branching random walks and related dynamics [6, 7, 28]. For additive rules such as ECA rules 90 and 150, the connection is indeed very close. We present the computation for ECA rule 90, which presents the simplest illustration of this correspondence.

Assume the initial defect is at the origin. As every defect spreads onto its two neighbors, the number of defects at $x = \alpha t$ is exactly the number of nearest-neighbor paths from the initial defect to x. This number is 2^t times the probability that the simple random walk S_t, started at the origin, ends at x. The large deviation theory [9] implies that, for $\alpha \in [-1, 1]$,

$$\frac{1}{t} \log \mathcal{P}(S_t = \alpha t) \sim \inf_{y \in \mathbb{R}} \left(-y\alpha + \log(\tfrac{1}{2}(e^y + e^{-y})) \right),$$

as $t \to \infty$. To explain the origin of this formula, we provide a computation that gives the upper bound. For $\alpha > 0$, and any $y > 0$,

$$\begin{aligned} \mathcal{P}(S_t = \alpha t) \approx \mathcal{P}(S_t \geq \alpha t) &= \mathcal{P}(\exp(y(S_t - \alpha t) \geq 1) \\ &\leq \mathcal{E}(\exp(y(S_t - y\alpha t)) = e^{-y\alpha t} \left(\frac{1}{2} e^y + \frac{1}{2} e^{-y} \right)^t. \end{aligned}$$

Now we take logarithms and divide by t, then optimize over $y > 0$, which agrees with optimization over $y \in \mathbb{R}$. After a short computation, we get:

$$L(\alpha) = \log 2 - \tfrac{1}{2}(1 + \alpha) \log(1 + \alpha) - \tfrac{1}{2}(1 - \alpha) \log(1 - \alpha).$$

Note that this expression equals $\log 2$ at $\alpha = 0$. By a similar calculation, the profile for ECA rule 150 equals

$$L(\alpha) = \log\left(1 + \alpha_0 + \frac{1}{\alpha_0}\right) - \alpha \log \alpha_0, \text{ where } \alpha_0 = \frac{\alpha + \sqrt{4 - 3\alpha^2}}{2(1-\alpha)}.$$

So, the MLE of rule 150 is $\lambda = \log 3$ and its corresponding MLE direction is 0.

For non-additive CAs, the random walks evolve in an environment determined by the CA trajectory. When the initial state is random, the Lyapunov profile is analogous to the quenched large deviation rates [28]. However, in our case the environment is highly correlated; as a result, there is no rigorous theory to date and a computational approach is in many cases the only one available.

3 LYAPUNOV PROFILES OF ELEMENTARY CELLULAR AUTOMATA

3.1 Experimental setup

In the remainder of this paper we will focus our attention on the 88 minimal elementary CAs as defined in [23]. For each of them, the propagation of defects emerging from a single defect was tracked for 5000 time steps in a one-dimensional system consisting of 10001 cells, unless specified otherwise. In this way, we mimicked a system of infinite size. All this was done for an ensemble $E = \{{}_e\xi_0 \mid e = 1, \ldots, 50\}$ of 50 different random initial configurations in order to account for the effects of the initial configuration on the defect propagation.

3.2 Defect shapes and density profiles

If one is only interested in the position of defects, one may confine the analysis to the so-called defect shape W. For that purpose, we introduce an auxiliary quantity $\delta(x,t)$, given by $\delta(x,t) = 1$ if $\Delta(x,t) > 0$ and $\delta(x,t) = 0$ otherwise, for every integer point x and time $t \geq 0$. We sometimes refer to the process δ_t as the percolation dynamics, as it tracks how defects spread through space. Using this notion, the defect shape W can now be defined as the closed subset $\mathbb{R}$ obtained by the following limit in the Hausdorff sense:

$$W = \lim_{t\to\infty} \frac{1}{t}\{x : \delta(t,x) = 1\} \tag{5}$$

provided the limit exists. If $\delta_t = \emptyset$ for some t, then we let $W = \emptyset$. We recall that as, the defect counts $\Delta(x,t)$ are integers, $L(\alpha)$ is either $-\infty$ or

nonnegative for every α. In fact, it is easy to show that

$$W = \{\alpha : L(\alpha) \geq 0\},$$

if W exists.

To capture information on the density of defects at a given site, we also introduce the defect density profile $\rho = \rho(\alpha)$ of a binary, one-dimensional CA that gives the proportion of defect sites in the direction $\alpha \in \mathbb{R}$, that is, on the rays $x = \alpha t$:

$$\rho(\alpha) = \lim_{t\to\infty} \frac{1}{t} \#\{(x,t) : t \geq 0, x = \lfloor \alpha t \rfloor, \delta(x,t) = 1\}, \tag{6}$$

provided that the limit exists.

It should be pointed out that the empirical Lyapunov profiles, defect shapes and defect density profiles constitute approximations of the ones defined in (3), (5) and (6), respectively, as the limit $t \to \infty$ in these equations is replaced by the evaluation of the expression at some large t. Still, for the sake of clarity and because the meaning will be clear from the context, we do not introduce a dichotomous notation to distinguish between the empirical constructs and the 'true' ones.

Figure 1 depicts the defect shapes and density profiles for ECA rules 22, 30, 106 and 150 that were obtained after 250 time steps for a system of 501 cells. Inspecting the defect shapes depicted in Figure 1, it is clear that these can be asymmetric and contain gaps. The former indicates that the directions of defect propagation are restricted and these restrictions are not symmetric, while the latter shows that some regions in space-time might block the propagation of defects. The defect density profiles shown at the right-hand side of Figure 1 give a better understanding of the spatially heterogeneous nature of defect spreading. Indeed, even within the regions of space-time where defects can propagate, this propagation strongly depends on the direction. Especially in the case of ECA rules 30 and 106, it is clear that the defect propagation can intensify less or more abruptly when moving into the region where defect propagation is possible towards the center of the defect cone. Moreover, as illustrated by the defect density profile of ECA rule 22, defects may 'die' even inside the defect cone, leading to a non-trivial defect density profile. The other rules in Figure 1 have a trivial density profile of 1 inside their defect shapes (though convergence can be quite slow). The asymptotic rate of spread of the damage front [8, 11, 22] for the ECA rule 22 has been estimated by Grassberger [15] to be about 0.77 (the rates are the same in both directions as this rule is symmetric). Figure 1 suggests that the asymptotic rate of

spread of defects for this rule is also around the same number and therefore that the two might agree. More extensive computations, however, provide considerable empirical evidence that the two are not asymptotically equal.

3.3 Statistics on Lyapunov profiles

Table 1 lists the following statistics for the for the 88 minimal ECAs: minimum ($\min_e \#W$), average ($\overline{\#W}$) and maximum ($\min_e \#W$) cardinality of the defect shape W, and the average ($\overline{L}$), minimum ($\min L$) and maximum ($\max L$) exponents in the empirical Lyapunov profile, together with the average relative center of mass of the empirical Lyapunov profile (γ). The values of the four latter statistics were obtained by computing them separately from every of the Lyapunov profiles obtained for an ensemble $E = \{{}_e\xi_0 \mid e = 1, \ldots, 50\}$ of 50 different random initial configurations, after which these values were averaged over the members of the ensemble E. The relative center of mass of the Lyapunov profile was computed as the sum of the cell indices times the corresponding number of defects, divided by the total number of defects times 5000.

Concerning the support of the defect cone, which is reflected by the minimum ($\min_e \#W$), average ($\overline{\#W}$) and maximum ($\min_e \#W$) cardinality of W, it is clear that the initial configuration plays an important role as $\min_e \#W$ and $\max_e \#W$ differ substantially for an important share of the investigated ECA rules, such as ECA rules 18, 22, 25 and 26. It means that some ECAs cannot evolve to their most stable state from certain initial configurations, as pointed out already in [5]. Essentially, the empirical results reported in Table 1 indicate that these rules are characterized by at least two attractors, a stable one implying a zero support of the defect shape and an unstable one giving rise to a non-zero support. Leaving aside the ECA rules for which $\#W$ is always 0, irrespective of the initial configuration, reversible ECAs (15 and 51) and essentially additive ECAs (60, 90, 105, 150, 170, 204) are the only ones for which the defect dynamics is not affected by the initial configuration. Either the initially introduced defect stays in the cell where it was introduced as the ECA evolves, which is distinctive for reversible ECAs and leads to $\#W = 1$ and $\lambda = 0$, or defects do spread – not necessarily symmetrically – in a way that is not affected by the initial configuration.

Listing the ECA rules for which the minimum, maximum and average support over the ensemble of initial configuration lie close to one another, i.e. ECA rules 30, 41, 45, 54, 56, 57, 60, 90, 105, 106, 110, 146 and 150, it becomes clear that there is only a handful of rules for which the support of the defect shape, and hence the width of the defect cone, does not strongly

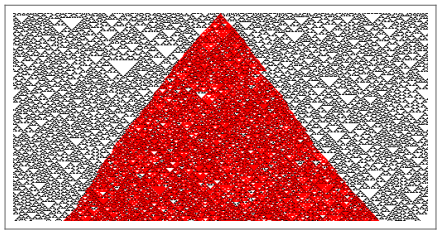

(a) Rule 22

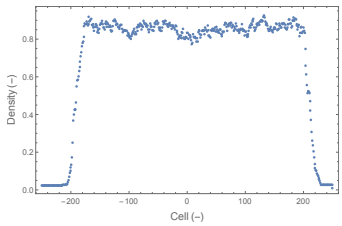

(b) Rule 22

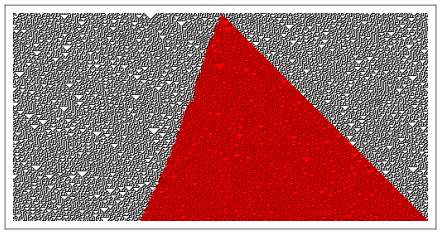

(c) Rule 30

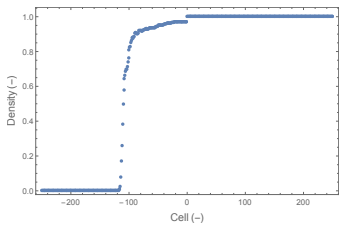

(d) Rule 30

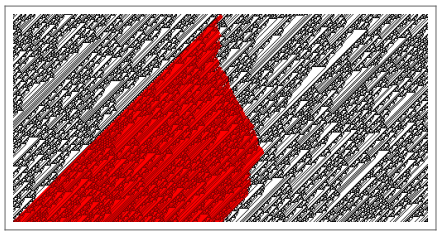

(e) Rule 106

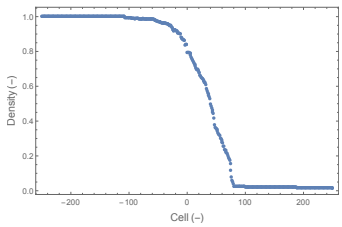

(f) Rule 106

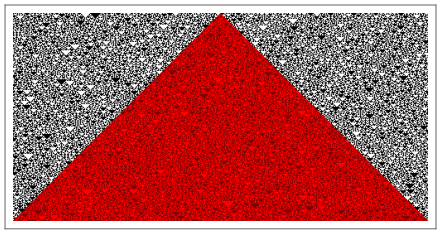

(g) Rule 150

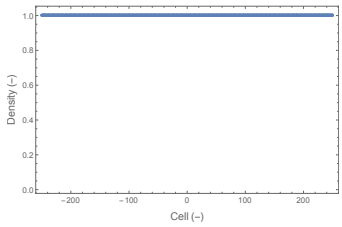

(h) Rule 150

FIGURE 1
Defect shapes (a, c, e, g) and density profiles (b, d, f, h) of ECA rules 22 (a, b), 30 (c, d), 106 (e, f) and 150 (g, h) that were obtained after 250 time steps for a system of 501 cells.

depend on the initial configuration. In light of Wolfram's classification, this list contains all Class 4 ECA rules, though the majority belong to Class 3, and two of them (ECA rules 56 and 57) are Class 2. This indicates that the Wolfram classification is not a good predictor for Lyapunov profiles.

Considering the exponents in the Lyapunov profiles, Table 1 confirms that ECA rules 105 and 150 are the most unstable as their average MLEs are $1.1 \approx \log(3)$. Given the fact that the defect shape of these rules is fully symmetric with respect to the initially perturbed cell ($\gamma = 0$), it also follows that its corresponding MLE direction is 0, which confirms the analytical result presented in Section 2.2. Further, it can be observed that for the ECA rules for which $\min_e \#W$ and $\max_e \#W$ differ more than 10 %, so whose defect propagation strongly depends on the initial configuration, and especially those whose maximum support does not span more than a few hundred cells, $\overline{L}$ is lower than 0.2 (e.g. ECA rules 5, 14, 19 and 23). This indicates that defect propagation is typically still very limited if such rules are evolved from an initial condition that hinders them to reach their most stable state. Yet, there are a few rules for which $\min_e \#W = 0$ and $\max_e \#W \leq 30$ (ECA rules 13, 28, 33, 72, 104, 156) that give rise to an average exponent $\overline{L}$ that is larger or equal than $0.41 \approx \log(\frac{3}{2})$, which means that the number of defects grows by at least about 50% at every time step even though the defect shape spans only a very narrow region in space-time. Here, ECA rule 72 stands out with $\max_e \#W = 3$, $\overline{L} = 0.62$ and $\lambda = 0.69 \approx \log(2)$, so it allows the number of defects almost to double if evolved from outside of the basin of attraction of a stable state with no defects. Concerning now those ECA rules involving a stable and unstable attractor for which the latter may imply a defect shape with a support that spans more than half of the light cone (ECA rules 6, 18, 22, 25, 26, 38, 122, 126, 134, 154), Table 1 indicates that these ECA rules lead to an average exponent $\overline{L}$ that is at least 0.22. Notably, the average exponent for some of these ECA rules (6, 25, 26, 38, 134, 154) is lower than or equal to the average exponent reached by those rules whose defect shape spans at most a few cells. This demonstrates that a wider defect shape does not necessarily imply a more intense defect propagation.

Inspecting the values of the average relative center of mass of the Lyapunov profiles in the right-most column of Table 1, it is clear that ECA rule 60 is the only one among the reversible and essentially additive ECA rules (15, 51, 90, 105, 150, 170, 204) that gives rise to an asymmetric profile. Apart from this, however, there seems to be no link between the symmetry of the Lyapunov profile, on the one hand, and the defect shape's support or the magnitude of the exponents in the profile, on the other hand. This is also

true for the four ECA rules in Wolfram's Class 4, two of which give rise to a profile that is skewed to the left (ECA rules 106 and 110), one to a profile that is skewed to the right (ECA rule 41) and one to a symmetric profile (ECA rule 54). Also in terms of any of the other statistics reported in Table 1 these four ECA rules do not stand out. This again indicates that the Wolfram classification is not a good predictor of Lyapunov shapes as it is merely based on the CA behavior in configuration space.

TABLE 1: Minimum ($\min_e \#W$), average ($\overline{\#W}$) and maximum ($\min_e \#W$) cardinality of W, and average ($\overline{L}$), minimum ($\min L$) and maximum ($\max L$) empirical Lyapunov exponent, averaged over an ensemble $E = \{{}_e\xi_0 \mid e = 1, \ldots, 50\}$ of 50 different random initial configurations, together with the average relative center of mass of the Lyapunov profile (γ).

Rule	$\min_e \#W$	$\overline{\#W}$	$\max_e \#W$	$\overline{L}$	$\min L$	$\max L$	γ
0	0	0	0	–	–	–	–
1	0	0.62	3	0.12	0.12	0.12	0
2	0	0.56	2	0	0	0	-1
3	0	0.78	2	0.11	0.11	0.11	0.5
4	0	0.8	2	0	0	0	0
5	0	0.64	2	0.07	0.07	0.07	0
6	0	4966.98	5584	0.41	0	0.55	-0.29
7	0	0.74	3	0.01	0.01	0.01	0.5
8	0	0	0	–	–	–	–
9	0	90.52	241	0.02	0	0.03	0.97
10	0	0.76	2	0	0	0	-1
11	0	2.8	11	0	0	0	1
12	0	0.88	2	0	0	0	0
13	0	0.54	3	0.48	0.48	0.48	0
14	0	3.82	191	0.05	0	0.09	-0.92
15	1	1	1	0	0	0	1
18	0	3715.8	5035	0.5	0	0.69	0
19	0	0.7	2	0.05	0.05	0.05	0
22	0	6082.28	6490	0.72	0.37	0.87	0
23	0	0.86	2	0.04	0.04	0.04	0
24	0	0.8	3	0	0	0	1
25	0	4825.78	5416	0.41	0.02	0.52	-0.18

Continued on next page

TABLE 1: (Continued)

Rule	$\min_e \#W$	$\overline{\#W}$	$\max_e \#W$	$\overline{L}$	$\min L$	$\max L$	γ
26	0	4381.48	6011	0.26	0	0.33	-0.45
27	0	2.44	9	0	0	0	0.5
28	1	3.94	13	0.44	0.44	0.44	0
29	1	2.58	6	0.06	0.06	0.06	0
30	6976	7059.06	7122	0.5	0	0.66	0.31
32	0	0	0	–	–	–	–
33	1	9.54	30	0.41	0.36	0.43	0
34	0	0.88	2	0	0	0	-1
35	0	8.6	60	0	0	0.01	0.5
36	0	1.78	4	0	0	0	0
37	2	19.62	46	0.34	0.3	0.35	0
38	0	4155	5497	0.4	0	0.54	-0.41
40	0	0	0	–	–	–	–
41	7864	7913.76	8017	0.63	0	0.86	0.02
42	0	0.9	2	0	0	0	-1
43	0	8.5	337	0.09	0	0.17	0.91
44	0	2.42	6	0.04	0.03	0.05	0
45	7327	7422.06	7501	0.56	0	0.72	0.21
46	0	3.42	16	0	0	0	-1
50	0	0.7	2	0.07	0.07	0.07	0
51	1	1	1	0	0	0	0
54	8239	8334.94	8447	0.54	0.13	0.74	0
56	285	419.92	526	0.09	0.04	0.1	0.87
57	7442	7496.66	7574	0.57	0.17	0.7	0
58	0	15.86	135	0.01	0	0.01	-0.99
60	5001	5001	5001	0.5	0	0.69	0.5
62	452	2479.36	2674	0.4	0.07	0.43	0.09
72	0	0.56	3	0.62	0.46	0.69	0
73	2	14.88	39	0.79	0.78	0.79	0
74	0	65.6	177	0.12	0.11	0.12	-0.82
76	0	1.16	2	0	0	0	0
77	0	0.7	2	0.1	0.1	0.1	0
78	0	1.66	6	0.18	0.15	0.23	0
90	5001	5001	5001	0.5	0	0.69	0
94	0	5.62	18	0.15	0.08	0.24	0

Continued on next page

TABLE 1: (Continued)

Rule	$\min_e \#W$	$\overline{\#W}$	$\max_e \#W$	$\overline{L}$	$\min L$	$\max L$	γ
104	0	0.82	3	0.48	0.05	0.69	0
105	10001	10001	10001	0.8	0	1.1	0
106	3800	4359.6	4926	0.55	0	0.71	-0.28
108	1	3.42	9	0.2	0.11	0.24	0
110	7204	7437.08	7519	0.48	0.05	0.65	-0.26
122	0	8600.52	9832	0.46	0.03	0.65	0
126	0	8400.9	9841	0.5	0.04	0.71	-0.01
128	0	0	0	–	–	–	–
130	0	1.1	5	0	0	0	-1
132	1	1.26	3	0	0	0	0
134	1	5548.6	5711	0.37	0	0.5	-0.23
136	0	0	0	–	–	–	–
138	0	1.22	9	0	0	0	-1
140	0	0.94	2	0	0	0	0
142	0	3.8	190	0.09	0	0.16	-0.92
146	5002	5021.92	5044	0.5	0	0.69	0
150	10001	10001	10001	0.8	0	1.1	0
152	0	2.16	12	0	0	0	1
154	1	3303.28	5580	0.22	0	0.29	-0.65
156	1	3.86	7	0.58	0.56	0.59	0
160	0	0	0	–	–	–	–
162	0	1.02	6	0	0	0	-1
164	1	2.86	10	0	0	0	0
168	0	0	0	–	–	–	–
170	1	1	1	0	0	0	-1
172	0	2.14	17	0.07	0.07	0.07	0
178	0	0.7	2	0.1	0.1	0.1	0
184	1	2.42	26	0.01	0.01	0.01	0
200	0	0.78	3	0.15	0.15	0.15	0
204	1	1	1	0	0	0	0
232	0	0.86	2	0.04	0.04	0.04	0

Figure 2 visualizes the Lyapunov profiles of the 23 ECA rules (6, 18, 22, 25, 26, 30, 38, 41, 45, 54, 57, 60, 62, 90, 105, 106, 110, 122, 126, 134, 146, 150 and 154) whose defect shapes, conditioned on the defect growth, consist of an interval of nonzero length. In agreement with the analytical result on

the Lyapunov profile of ECA rule 150 presented in Section 2.2 and the statistics listed in Table 1, the Lyapunov profile of this rule is positive everywhere and reaches its maximum where the defect was initially introduced. Figure 2 demonstrates that the skewedness of ECA rule 106 to the left, as could already be inferred from its $\gamma = -0.28$ in Table 1, is so extreme that all of its real-valued exponents lie to the left-hand side of the initially perturbed cell. This implies that cells to the right of this cell remain unaffected, and hence they evolve as they would in absence of any defect. A similar reasoning holds for ECA rules 60 and 62, which give rise to a peculiar Lyapunov profile. ECA rules 6, 25, 26, 30, , 38, 41, 45, 62, 100, 134 and 154 are also characterized by a skewed Lyapunov profile, though the support of the defect shape now extends to the left and right of the initially perturbed cell. The Lyapunov profile of ECA rule 22 is symmetric, as could be expected on the basis of its defect shape and density profile shown in Figure 1, but defects do not succeed in propagating on average one cell per time step at either side of the initially perturbed cell. More specifically, the average asymptotic rate of defect propagation is about 0.74, as the right-most cell with a positive Lyapunov exponent has index 3753 (cfr. Fig. 2), which is lower than the asymptotic rate of spread of the damage front as reported by Grassberger [15].

When comparing the magnitudes of the exponents in the Lyapunov profiles depicted in Figure 2, and recalling that the Lyapunov profile of ECA rule 150 represents the upper bound on defect propagation in ECAs, it can be seen that the defect propagation is the most intense in the case of symmetric Lyapunov profiles. We also point out that ECA rule 106 has a particularly notable defect dynamics, as already suggested by Figure 1. A closer inspection (see Figure 2) reveals that its empirical Lyapunov profile converges very slowly, and exhibits significant fluctuations; for example there are several local minima where the propagation of defects is less intense.

Figure 2: Lyapunov profiles after 5000 time steps for a system of 10001 cells of the 23 ECA rules whose defect shapes, conditioned on the defect growth, consist of an interval of nonzero length.

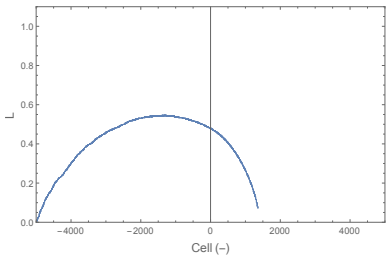

(a) Rule 6

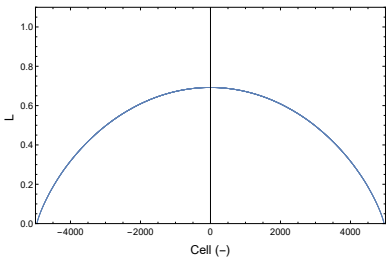

(b) Rule 18

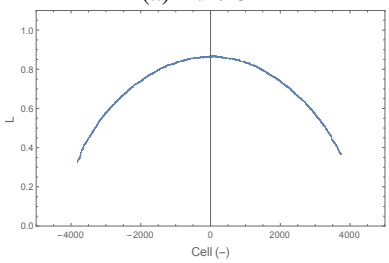

(c) Rule 22

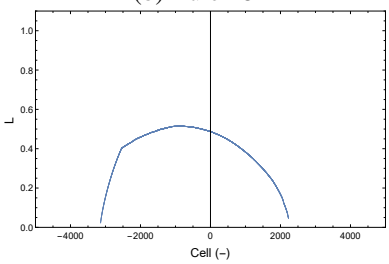

(d) Rule 25

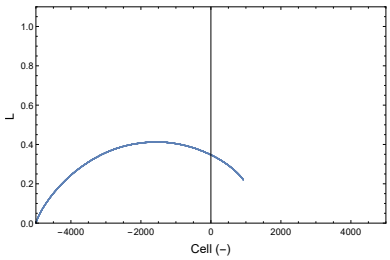

(e) Rule 26

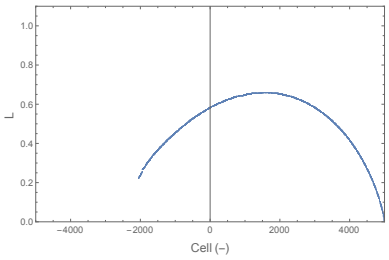

(f) Rule 30

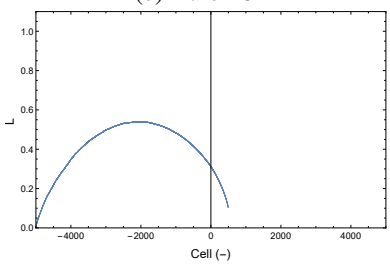

(g) Rule 38

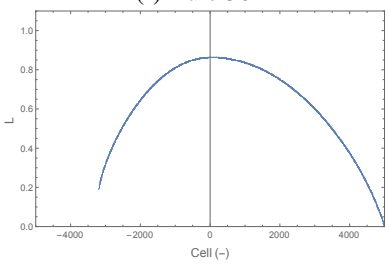

(h) Rule 41

Figure 2: continued

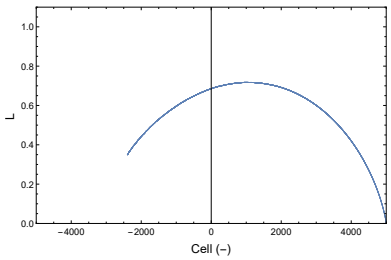

(i) Rule 45

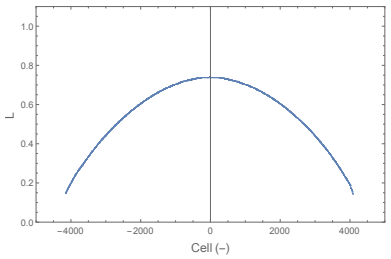

(j) Rule 54

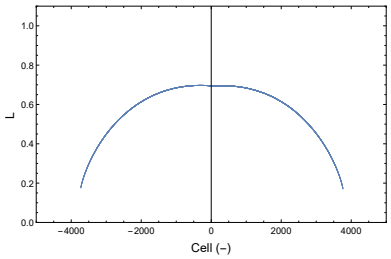

(k) Rule 57

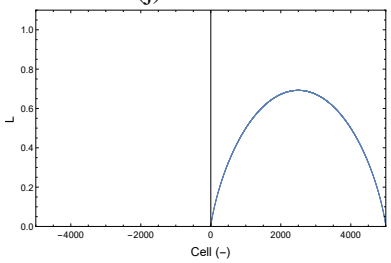

(l) Rule 60

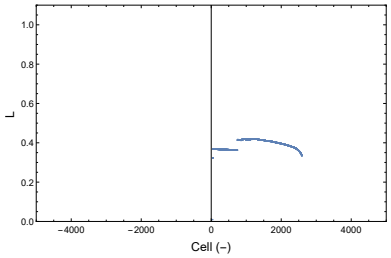

(m) Rule 62

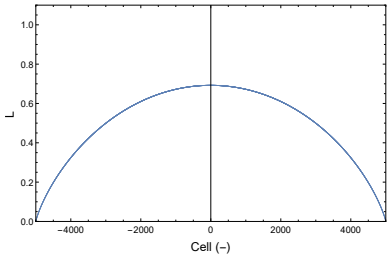

(n) Rule 90

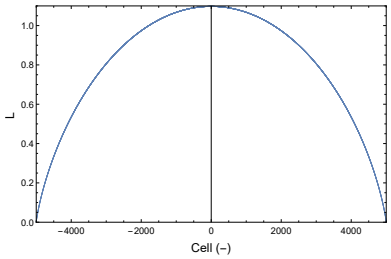

(o) Rule 105

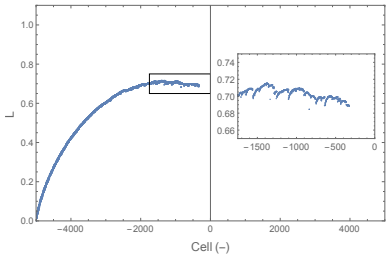

(p) Rule 106

Figure 2: continued

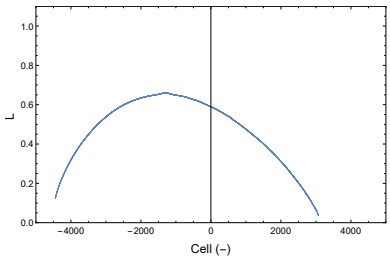

(q) Rule 110

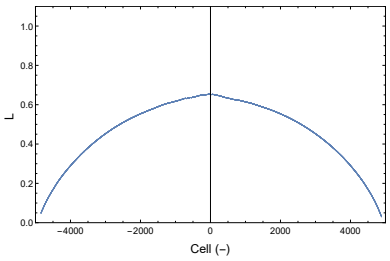

(r) Rule 122

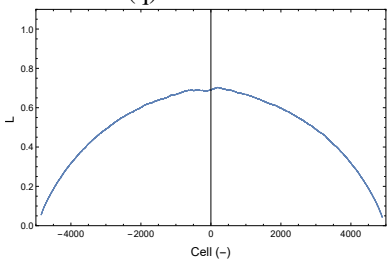

(s) Rule 126

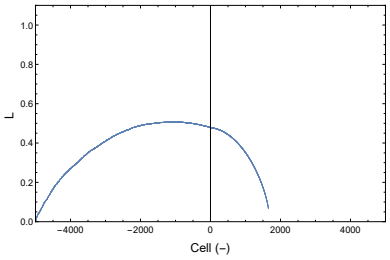

(t) Rule 134

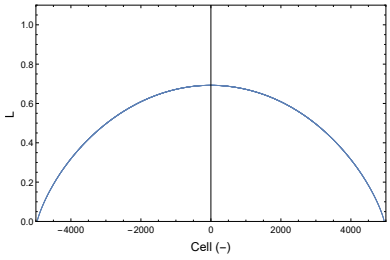

(u) Rule 146

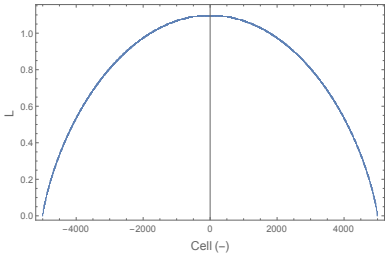

(v) Rule 150

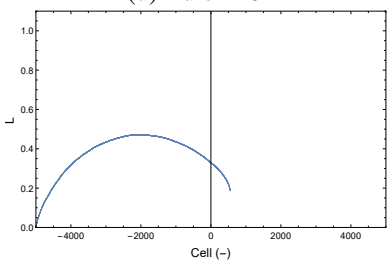

(w) Rule 154

4 SUMMARY AND CONCLUSIONS

In this paper we introduced a tool by which the spatial variation of perturbations of CA trajectories may be studied. Our approach is based on that of Bagnoli et al. [5], with one crucial change in perspective: we consider the CA evolution on the entire infinite lattice $\mathbb{Z}$. The resulting defect dynamics starts from a localized seed of a single defect, and subsequently propagates defects which are able to perturb the CA trajectory. As time increases, the resulting set of defects shows a considerable spatial variation, even at the exponential level, and the resulting exponential rates on the space-time rays are gathered into the Lyapunov profile. In particular, the maximum of this profile recovers the MLE introduced by Bagnoli et al. [5], and its location defines the principal direction of spread of defects. Finally, the defect shape — the set on which the profile is finite — measures the extent of perturbation effects. The sites that contain at least one defect may occupy only a proportion of the defect shape, leading to a nontrivial defect density profile.

We conducted an extensive, mostly empirical, analysis of this object for the ECA, for which the evolution is started from a random initial state generated by independent fair coin flips. We briefly summarize our main conclusions below.

- The defect dynamics are the simplest for additive (and closely related) CA, where they are independent of the initial state and Lyapunov profiles can be computed exactly using theory of large deviations. These could be used as upper bounds for non-additive CA.

- For essentially non-additive rules, the defect dynamics depend on the initial state. For a few rules, the Lyapunov profile (which is a limiting object) is however independent of the initial state; this includes chaotic rules such as 30 or 106. For most rules, the profile is dependent on the initial state (i.e., is random).

- There are simple rules, such as 8, for which the defects always die out, leading to an empty defect shape.

- For many other rules (e.g., rule 22), defects may still die out by chance at the beginning. Assuming defect survival, the defect shape varies widely across the rules, consisting sometimes of a single point (e.g., 0.5 for rule 3), sometimes more than half of the light cone (e.g., rules 6 and 22).

- Asymmetry in the CA rule gives rise to the dramatic asymmetry of its Lyapunov profile; perhaps the best example is rule 106.

5 ACKNOWLEDGMENTS

An early version of this paper appeared in the local proceedings of AUTOMATA 2014 [2]. The present version adds formal definitions, and considerably extends the empirical and theoretical analysis. We thank the referees for the original proceedings and for this version for many helpful comments that significantly improved the paper. We gratefully acknowledge the assistance of STEVIN Supercomputer Infrastructure at Ghent University, funded by Ghent University, the Flemish Supercomputer Center (VSC), the Hercules Foundation and the Flemish Government - department EWI. Janko Gravner was partially supported by the Simons Foundation Award #281309 and the Republic of Slovenia's Ministry of Science program P1-285.

REFERENCES

[1] J. M. Baetens and B. De Baets. (2010). Phenomenological study of irregular cellular automata based on Lyapunov exponents and Jacobians. *Chaos*, 20:033112.

[2] J.M. Baetens and J. Gravner. (July 2014). Introducing Lyapunov profiles of cellular automata. In T. Isokawa, K. Imai, Matsuin N., F. Peper, and H. Umeo, editors, *Proceedings of the 20th International Workshop on Cellular Automata and Discrete Complex Systems (AUTOMATA 2014) - Exploratory Papers*, pages 133–140, Himeji, Japan.

[3] J.M. Baetens and J. Gravner. (2016). Stability of cellular automata trajectories revisited: branching walks and lyapunov profiles. *Journal of Nonlinear Science*, 26:1329–1367.

[4] F. Bagnoli and R. Rechtman. (2009). Thermodynamic entropy and chaos in a discrete hydrodynamical system. *Phys. Rev. E*, 79:041115.

[5] F. Bagnoli, R. Rechtman, and S. Ruffo. (1992). Damage spreading and Lyapunov exponents in cellular automata. *Phys. Lett. A*, 172:34–38.

[6] J. D. Biggins. (1995). The growth and spread of the general branching random walk. *Ann. Appl. Probab.*, 5:1008–1024.

[7] M. Bramson, P. Ney, and J. Tao. (1992). The population composition of a multitype branching random walk. *Ann. Appl. Probab.*, 2:519–765.

[8] M. Courbage and B. Kamiński. (2006). Space-time directional Lyapunov exponents for cellular automata. *Journal of Statistical Physics*, 124:1499–1509.

[9] A. Dembo and O. Zeitouni. (1998). *Large Deviations Techniques and Applications*. Springer, Heidelberg, Germany, 2 edition.

[10] A. Deutsch and S. Dormann. (2005). *Cellular Automaton Modeling of Biological Pattern Formation: Characterization, Applications, and Analysis*. Birkhäuser, Bonn, Germany.

[11] M. Finelli, G. Manzini, and L. Margara. (1998). Lyapunov exponents versus expansivity and sensitivity in cellular automata. *J. Complexity*, 14:210–233.

[12] M. Gardner. (1971). Mathematical games: The fantastic combinations of John Conway's new solitaire game 'Life'. *Scientific American*, 223:120–123.

[13] Michael J. Gibson, Edward C. Keedwell, and Dragan A. Savi? (2015). An investigation of the efficient implementation of cellular automata on multi-core {CPU} and {GPU} hardware. *J. Parallel Distrib. Comput.*, 77:11 – 25.

[14] P. Grassberger. (1984). Chaos and diffusion in deterministic cellular automata. *Phys. D*, 10:52–58.

[15] P. Grassberger. (1986). Long-range effects in an elementary cellular automaton. *J. Statist. Phys.*, 45:27–39.

[16] A. Ilachinski, editor. (2001). *Cellular Automata. A Discrete Universe*. World Scientific, London, United Kingdom.

[17] C.G. Langton. (1990). Computation at the edge of chaos. *Phys. D*, 42:12–37.

[18] G.J. Martínez. (2013). A note on elementary cellular automata classification. *J. Cell. Autom.*, 8:233–259.

[19] J.A. Parsons and M.A. Fonstad. (2007). A cellular automata model of surface water flow. *Hydrological Processes*, 21:2189–2195.

[20] T. Reichenbach, M. Mobilia, and E. Frey. (2007). Mobility promotes and jeopardizes biodiversity in rock-paper-scissors games. *Nature*, 448:1046–1049.

[21] M.A. Shereshevsky. (1991). Lyapunov exponents for one-dimensional cellular automata. *J. Nonlinear Sci.*, 2:1–8.

[22] P. Tisseur. (2000). Cellular automata and Lyapunov exponents. *Nonlinearity*, 13:1547–1560.

[23] G.Y. Vichniac. (1990). Boolean derivatives on cellular automata. *Physica D*, 45:63–74.

[24] J. von Neumann. (1951). The general and logical theory of automata. In L. A. Jeffres, editor, *Cerebral Mechanisms in Behaviour. The Hixon Symposium*, pages 1–41, Pasadena, United States. John Wiley & Sons.

[25] S. Wolfram. (1983). Statistical mechanics of cellular automata. *Reviews of Modern Physics*, 55:601–644.

[26] S. Wolfram. (1984). Universality and complexity in cellular automata. *Phy. D*, 10:1–35.

[27] A. Wuensche and M. Lesser. (1992). *The Global Dynamics of Cellular Automata*, volume 1. Addison-Wesley, London, United Kingdom.

[28] A. Yilmaz. (2009). Quenched large deviations for random walk in a random environment. *Commun. Pure and Appl. Math.*, 62:1033–1075.